ELSEVIER

Biophysical Chemistry 113 (2005) 155–160

Biophysical Chemistry

www.elsevier.com/locate/bpc

NMR study of the folding–unfolding mechanism for the thrombin-binding DNA aptamer d(GGTTGGTGTGGTTGG)

Xi-an Mao*,[1], William H. Gmeiner

Biochemistry Department, Wake Forest University School of Medicine, Medical Center Blvd, Winston-Salem, NC 27157-1016, USA

Received 18 August 2004; received in revised form 9 September 2004; accepted 9 September 2004
Available online 29 September 2004

Abstract

Hydrogen exchange rates of the imino protons of the thrombin-binding 15 mer DNA aptamer d($G_1G_2T_3T_4G_5G_6T_7G_8T_9G_{10}G_{11}T_{12}T_{13}G_{14}G_{15}$) in the presence of Sr^{2+} were measured. In the temperature range 15–35 °C, the exchange rates of the eight iminos in the quadruplex core were not uniform, with the G_2, G_{11} and G_{15} iminos exchanging faster, the G_1, G_5, G_{10} and G_{14} iminos exchanging slower, and the G_6 imino exchanging at a medium rate. In the quadruplex G_1, G_5, G_{10} and G_{14} adopted syn glycosidic conformation, while G_2, G_6, G_{11} and G_{15} adopted anti-conformation. It was found that the four slowly exchanging iminos, which were all the syn-iminos, happened to be located in the TT loops that were not easy to open to the solvent. The anti-iminos exchanged faster, but the G_6 imino exchanged slower than other anti-iminos, because its hydrogen bond with the $G_{10}O6$ was stabilized by the TGT loop. The fact that the G_6 imino exchanged at a faster rate than those syn-iminos in the TT loops suggested that the TGT loop was less stable than the TT loops. Unfolding mechanism for the quadruplex was thus proposed: The quadruplex first uncoupled the three base pairs: G_1–G_{15}, G_2–G_{14} and G_5–G_{11}, which were not protected by any loops. Then it opened the TGT loop. Finally, it opened the TT loops and the sequence became an unstructured random coil that exchanged with the quadruplex conformation. The conformational exchange between the quadruplex and random coil had been detected.

Keywords: NMR; Hydrogen exchange rates; Thrombin-binding DNA aptamer; Folding–unfolding mechanism

1. Introduction

Folding and unfolding of nucleic acids are of great importance in understanding their biological nature and have attracted much attention. It is known that the folding and unfolding processes of some nucleic acids are in milliseconds [1], which fall into the chemical shift time scale of NMR. NMR has therefore been used to study the conformational exchange of DNA and RNA, basically, through exchange spectroscopy [2] or hydrogen exchange rate detection [3]. Zhou et al. [4] observed interconversion between two conformations of an arylamine-modified 12 mer duplex DNA. Overmars and Altona [5] quantitatively measured the exchange rates between different conformations of a single-stranded 36 mer DNA that had a number of Holiday junctions. Recently, Phan and Patel [6] studied the chemical exchange between the parallel and antiparallel G-quadruplexes of a human telomeric DNA sequence. Here, we report the result of NMR study of the folding–unfolding dynamics of the thrombin-binding DNA aptamer (TBA) in the presence of divalent metal ion Sr^{2+}.

The DNA aptamer, with the sequence d($G_1G_2T_3T_4G_5G_6T_7G_8T_9G_{10}G_{11}T_{12}T_{13}G_{14}G_{15}$), was identified in 1992 [7], which showed strong binding ability to thrombin. Since then, this DNA has been intensively studied [8–22] because of its potential application in drug design [23]. NMR studies [9–12,16,17,22] have revealed that, in the presence of metal ions that fit the geometry of the quadruplex, the TBA folds into a chair-like conformation

* Corresponding author. Tel.: +1 216 368 0565; fax: +1 216 368 3952.
E-mail address: xian.mao@cwru.edu (X. Mao).
[1] Present address: Department of Physiology and Biophysics, Case Western Reserve University, School of Medicine, Cleveland, OH 44106-4970, USA.

0301-4622/$ - see front matter © 2004 Elsevier B.V. All rights reserved.
doi:10.1016/j.bpc.2004.09.003

as depicted in Fig. 1. Although the quadruplex stability may differ when different metal ions are present [18], our recent study [22] revealed that the Sr^{2+}-stabilized TBA quadruplex adopted the same topology as K^+-stabilized quadruplex. Eight guanines, which adopt alternatively anti–syn–anti–syn glycosidic conformations, form two tetrads stacked together and linked by three loops, T_3T_4, $T_7G_8T_9$ and $T_{12}T_{13}$. Each guanine in the quadruplex core plays a role as a hydrogen donator (offering imino H1 and amino H21) as well as a hydrogen acceptor (using O6 and N7 to accept hydrogen), forming four hydrogen bonds with two neighbor guanines. The interactions of the aptamer with some mono- and divalent metal ions, including Mn^{2+} [15], Pb^{2+} [17,19] and Sr^{2+} [18,22], have also been studied. Dynamic information about this aptamer has also received attention [21].

In this work, we studied the hydrogen exchange rates of the iminos of TBA. We found that at room temperatures, some hydrogen bonds were more stable than others. The hydrogen bonds stabilized by the TT loops were most stable, the hydrogen bonds stabilized by the TGT loop went second, and the other hydrogen bonds that were out of protection of any loops were least stable. Thus, the folding and unfolding of the quadruplex are easily understood. The loops, particularly the TT loops, played a key role in folding the DNA to a quadruplex conformation.

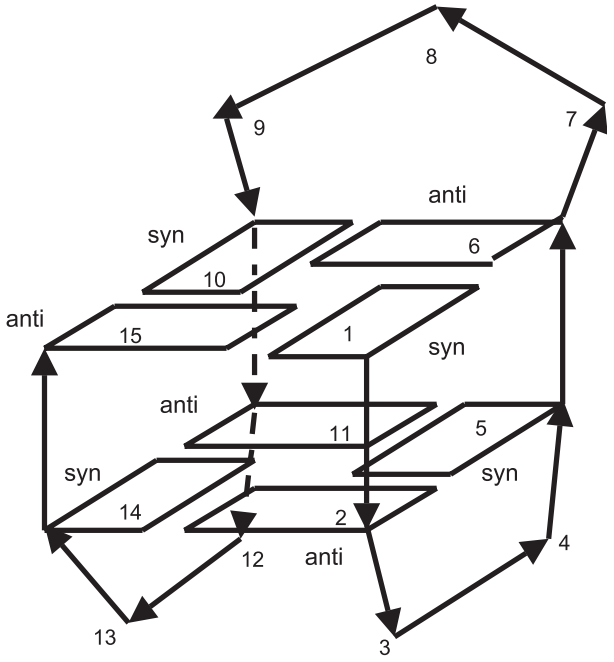

Fig. 1. Chair-like quadruplex conformation of the 15 mer DNA d($G_1G_2T_3T_4G_5G_6T_7G_8T_9G_{10}G_{11}T_{12}T_{13}G_{14}G_{15}$), in which eight guanines (G_1, G_2, G_5, G_6, G_{10}, G_{11}, G_{14} and G_{15}) form two stacked tetrads as the chair body, which adopted alternative syn–anti–syn–anti glycosidic conformations, four thymines (T_3, T_4, T_{12} and T_{13}) form two TT loops as the chair legs, and the other two thymines (T_7 and T_9) and a guanine (G_8) form a TGT loop as the chair back. Each guanine in the quadruplex core forms four hydrogen bonds, using four atoms H1, H21, O6 and N7, with its two neighbor guanines.

2. Materials and methods

Sample preparation and NMR experiments were basically described in our previous paper [22]. TBA was prepared using DNA synthesizer and was purified using HPLC. Unfolded TBA was brought into folded quadruplex by titrating the sample with $SrCl_2$. The final composition of the sample for quantitative kinetics study was 2:1 in metal/DNA ratio in 90% H_2O/10% D_2O, and the concentration of TBA was 1 mM at pH 5.9.

NMR experiments were performed on a Bruker Avance 600 spectrometer with a triple resonance probe. Chemical shifts were referenced to DSS (2,2-dimethyl-2-silapentane-5-sulfonic acid). For the evaluation of the hydrogen exchange rate between the imino protons of guanines and the water protons, the effective relaxation rates, $R_{1,\mathrm{eff}}$, the steady-state magnetizations, M_{ss}, and the equilibrium magnetizations, M_0, were measured independently. $R_{1,\mathrm{eff}}$ values were measured using the inversion recovery method with water selectively (using 1 ms Gaussian shaped pulse for 90° excitation) flipped back. In this case, the detected $R_{1,\mathrm{eff}}$ was the combination of the relaxation rate, R_1, with the hydrogen exchange rate, k_{ex}, i.e.,

$$R_{1,\mathrm{eff}} = k_{\mathrm{ex}} + R_1 \tag{1}$$

The steady-state magnetization intensities, M_{ss}, were evaluated in the presaturation experiment with long preirradiation time (6 s). The saturation percentage is related to k_{ex} and R_1 by

$$\frac{M_{\mathrm{ss}}}{M_0} = \frac{R_1}{k_{\mathrm{ex}} + R_1} \tag{2}$$

The equilibrium intensities, M_0, were obtained using water flip-back method. By combination of Eqs. (1) and (2), the hydrogen exchange rates, k_{ex}, were evaluated.

NOESY spectra [24] in 90% H_2O were recorded using standard three pulse sequence using Watergate [25] for water suppression and 300 ms for magnetization mixing. ROESY experiment [26] was conducted on another sample with the metal-to-DNA ratio of 0.3:1 in 100% D_2O. The ROESY spin locking time was 50 ms at the power level of 9900 Hz.

3. Results and discussion

Folded DNA usually shows countable imino signals in 1D NMR spectrum. In the low-field region between 11.5 and 12.3 ppm, the TBA quadruplex showed eight imino signals with somewhat overlapping (Fig. 2), with the four iminos of the anticonformation guanines (G_2, G_{15}, G_{11} and G_6) at the lower field and the four syn-iminos (G_1, G_{10}, G_5, and G_{14}) at the upper field. In the water flip-back experiment, the eight imino signals had nearly equal intensities (Fig. 2A). In the water presaturation experiment after long

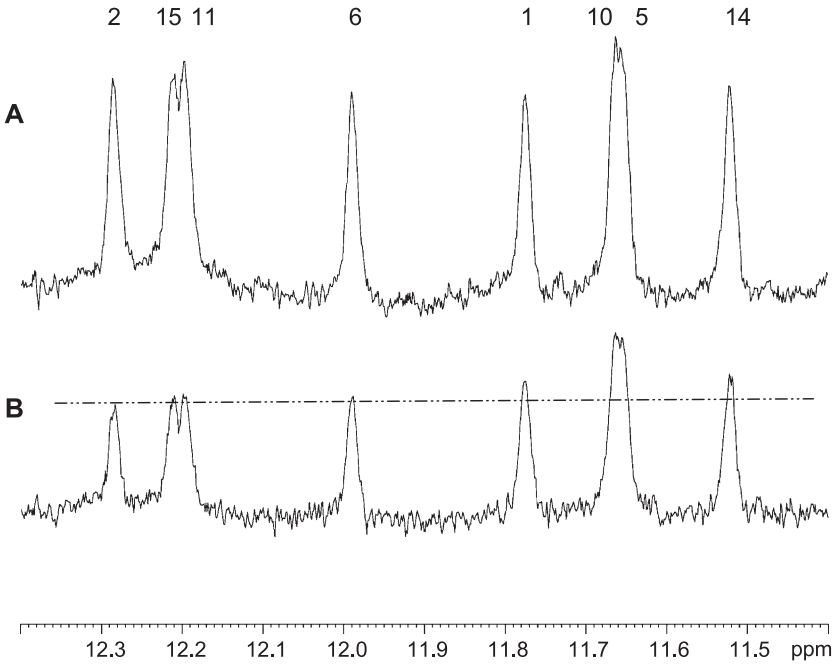

Fig. 2. Imino region (11.5–12.3 ppm) of the 1D spectra of the 15 mer DNA at 25 °C. (A) Spectrum with water flip back. Eight iminos show similar intensities. (B) Spectrum with water presaturation. Eight iminos have different intensities, with the down-field three iminos apparently weaker than the up-field four iminos. The G_6 imino (at 11.98 ppm) has medium intensity. For comparison of the intensities, a dashed horizontal line is drawn in (B).

preirradiation (6 s), however, they showed different intensities. The three anti-iminos at the lowest field apparently had lower intensities than the four syn-iminos at the upper field, while the imino intensity of G6, which also adopted anti-glycosidic conformation, was slightly lower than the syn-iminos but higher than the other three anti-iminos.

The lower intensities in the presaturation experiment (Fig. 2B) as compared to the intensities in the water flip-back experiment (Fig. 2A) indicated that water saturation had been transferred to the iminos due to hydrogen exchange between the imino and water protons. But the unequal intensities in the presaturation experiments implied that water saturation had been transferred to the iminos with unequal degrees. According to Eq. (2), not only the exchange rate but also the relaxation rate affected the steady-state intensity. For the lower steady-state intensities of the three anti-iminos shown in Fig. 2B, either of the two possibilities alone could be the reason: (1) Their relaxation rates were relatively lower; (2) Their exchange rates were relatively higher. Because proton relaxation is predominated by dipole–dipole interaction, only the protons nearby need to be considered when the imino relaxation rates are compared. In the quadruplex core, all eight imino protons had the same proton environments, as can be seen from one of the tetrads in Fig. 3: Each core imino had two aminos (in the same base) as its nearest neighbors and three iminos (in other bases) in its next outer neighborhood. If we do not consider the difference in glycosidic conformation, the four iminos in the tetrad were not distinguishable and their relaxation rates should be the same. The difference in glycosidic torsion angles did influence the environments of the core iminos. But because the ribose protons were in the far distance (the nearest ribose proton is about 7–8 Å away), their effect may be negligible. If they do need to be considered, the ribose protons were all closer to the same base imino proton in anticonformation than in syn-conformation, in average about 0.5–0.8 Å shorter in distance. The anti-iminos should relax faster than the syn-iminos. Detailed analyses of the quadruplex structure [22] showed that the presence of the other tetrad did not favor the relaxation of any particular imino either. Therefore, the

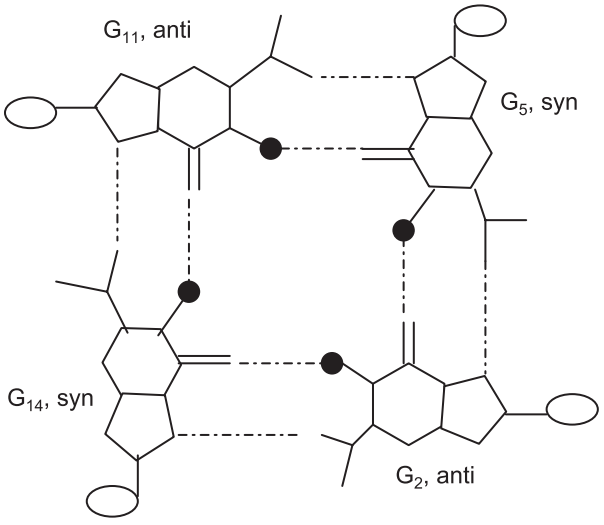

Fig. 3. One of the two tetrads in the quadruplex core. The filled circles represent the hydrogen-bonded iminos. The other tetrad has exactly the same topology.

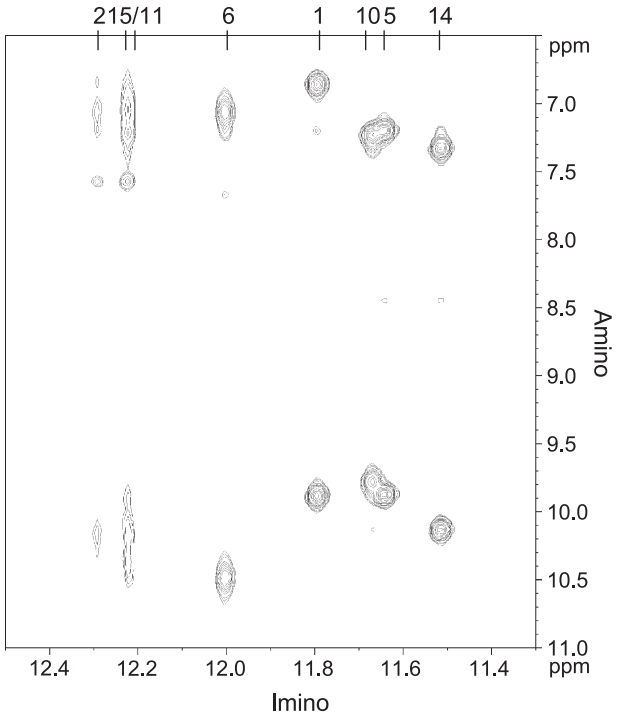

Fig. 4. Imino–amino correlation region of a NOESY spectrum with a mixing time of 300 ms at 25 °C. Although the iminos have similar linewidths, the amino linewidths are far from uniform. The three residues, G_2, G_{15} and G_{11}, have very broadened aminos that could merely be detected. The G_6 guanine has medium linewidth for its aminos. The four pairs of syn-aminos are sharp. The linewidths of the aminos are in agreement with the intensities of the iminos shown in Fig. 2B, and both give the same information: the easiness for the exchangeable protons to open to the solvent was in the order: G_2~G_{11}~G_{15}>G_6>G_1~G_5~G_{10}~G_{14}.

lower steady-state intensities of the three anti-imino protons in Fig. 2B were not due to the presumably slower relaxation. The first possibility is not relevant and can be ruled out.

The exchange rates, however, could be faster for the three anti-iminos, and the faster exchange rates should be the pronounced reason for their lower intensities in the saturation transfer experiment. It is well known that hydrogen exchange rate depends on how easy the proton is open to the solvent [27]. A glance at the quadruplex would not help find particular hindrance for a specific imino proton to open to water. However, by carefully inspecting the topology presented in Fig. 1, it is not difficult to find that the three faster exchanging iminos of the antiguanines, G_2, G_{15} and G_{11}, happen to sit at positions that were easier to open to solvent than the other five iminos that were all inside the loops. It is very likely that the three anti-iminos exchanged faster than the other iminos.

If the three iminos exchanged faster, the three base pairs, G_2–G_{14}, G_{15}–G_1 and G_{11}–G_5, should be more easily open than other base pairs, and correspondingly the aminos of G_2, G_{15} and G_{11} should also exchange faster than other aminos. The NOESY spectrum in 90% H_2O clearly demonstrated that the open-to-solvent rates for the three abovementioned base pairs were higher. In the imino–amino correlation region, the NOE cross peaks for the amino groups in the three anti-guanines were seriously broadened (Fig. 4), as compared to the NOE peaks for the other five amino groups. There is no doubt that the broadening resulted from faster exchange which in turn resulted from the faster open-to-solvent rate [27]. The line broadening in NOESY spectrum was in full agreement with the saturation transfer in presaturation experiment.

Quantitative results of the exchange rates are given in Fig. 5. At 25 °C in particular, the exchange rates for the three faster exchanging iminos were around 0.23 s^{-1}, for the slower exchanging iminos, the exchange rates were around 0.15 s^{-1}, while the exchange rate for G6 imino was about 0.18 s^{-1}. Although the difference between the exchange rates was small, it was beyond the experimental error which was estimated to be $\pm$0.02 s^{-1}. In the temperature range from 15 to 35 °C, the three anti-iminos consistently showed higher exchange rates than the other five iminos. But when the temperature was further elevated, all iminos tended to have similar exchange rates. This means that at higher temperatures, the loops also opened very rapidly.

It is worthwhile noticing that in all three figures (Figs. 2, 4 and 5), the imino and amino protons of G_6, which was also an anti-guanine, exchanged with water at a medium rate. This suggested that the $T_7G_8T_9$ loop was relatively easier to open than the other two loops, T_3T_4 and $T_{12}T_{13}$. Or in another word, the TGT loop was less stable than the TT loop. Loop stability is a topic of great interest in nucleic acids studies. Our data clearly indicate that, under the experimental conditions, the TT loops, although extremely short, were most difficult to unzip.

The apparent faster exchange for G_2, G_{11} and G_{15} iminos, the medium exchange for G_6 and the slower exchange for G_1, G_5, G_{10} and G_{14} enable us to propose an unfolding mechanism for the TBA in the presence of Sr^{2+}. The

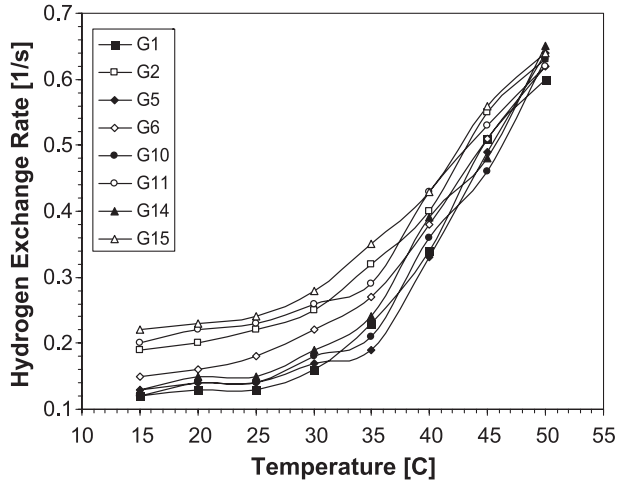

Fig. 5. Hydrogen exchange rates for the eight imino protons in the quadruplex core. The four syn-iminos, G_1, G_5, G_{10} and G_{14}, all in filled symbols, exchange slower than other iminos (in open symbols) in the temperature range from 15 to 35 °C. The G_6 imino always exchanges at a medium rate, as compared to the syn-iminos and other anti-iminos.

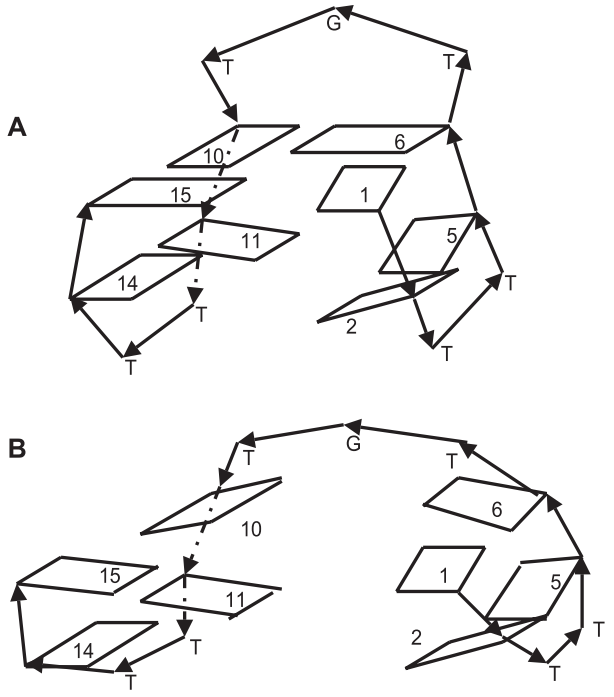

Fig. 6. Sketch showing possible intermediate conformations during the quadruplex unfolding. In conformation (A), the hydrogen bonds, which hold the G_{15}–G_1, G_{11}–G_5 and G_{14}–G_2 base pairs and have not been protected by loops, break, and the lower tetrad is split into two parts, while the upper tetrad cracks at the front edge. In conformation (B), the G_6–G_{10} base pair breaks and the TGT loop is open. The DNA is ready to unzip its TT loops and is going to finish the loop-to-coil transition.

hydrogen bonds outside the loops broke at first. During this process, there was no anti–syn conformation exchange, because the inner-loop hydrogen bonds were still holding. The lower tetrad was split into two parts, while the upper tetrad was cracked at the front edge with the back edge still in "good" shape, because the $T_7G_8T_9$ loop can stabilize the hydrogen bonds between G_6 and G_{10}. The quadruplex "chair" began to collapse in a way shown in Fig. 6A. Then, the G_6–G_{10} base pair was difficult to maintain and broke afterwards (Fig. 6B). Finally, all hydrogen bonds frayed away. The DNA underwent a hairpin-to-coil transition. There were no base pairs in the sequence and the DNA adopted unstructured conformation or random coil conformation. The DNA residues could undergo anti–syn exchange freely.

Our DNA quadruplex was stabilized by Sr^{2+} ion. An interesting question would be that, is the unfolding mechanism dependent on metal ions? The answer is no. Our further study of the TBA in the presence of potassium ion showed similar results in both presaturation and NOESY experiments (data not shown) as in the presence of Sr^{2+}. This means that the mechanism of unfolding of the quadruplex is independent of metal ions.

It should be pointed out that the conformations shown in Fig. 6 were possible intermediates during the TBA unfolding. They were not stable enough to give any NMR signals. They had only very short lifetimes. But the random coil conformation was stable in the solution. In a sample where the metal-to-DNA titration was not complete (about 0.3:1),

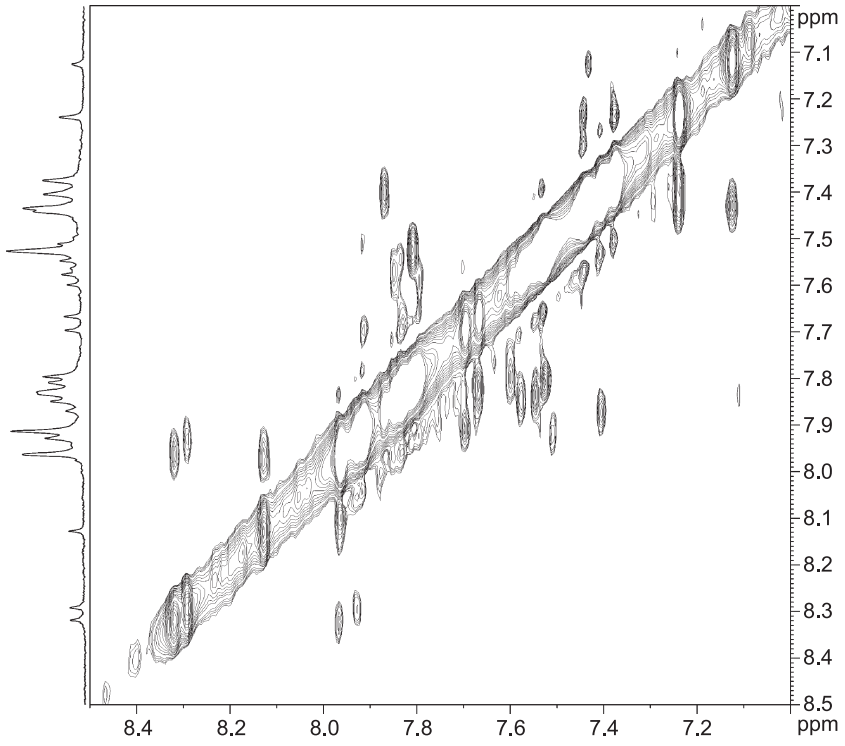

Fig. 7. Base region of a ROESY spectrum with a mixing time of 50 ms. On the left side, the 1D spectrum is presented, where two sets of signals can be distinguished with the intensity ratio approximately 3:1. The stronger signals, which are crowded in a narrow range, are assigned to the random coil conformation. The more dispersed weaker signals are assigned to the quadruplex conformation. The cross peaks, which show the same phase with the diagonal peaks, are due to the conformational exchange between the random coil conformation and the quadruplex conformation.

the random coil conformation showed distinct resonances which were easily distinguished from the quadruplex resonances, and the quadruplex signals showed exchange cross peaks with the random coil signals in a ROESY spectrum (Fig. 7). While the folded quadruplex base signals dispersed in a wide range from 7.1 to 8.3 ppm, the unstructured random coil base signals had much narrower resonance range. The nine guanines were crowded in the 7.8–7.96 ppm range and the six thymines were in the 7.37–7.52 range (see the projection spectrum in Fig. 7). Quantitative analysis of the ROESY exchange cross peaks yielded conformational exchange rates (date not shown), which were always smaller than the imino hydrogen exchange rates. This can be rationalized that conformational exchange happened only when all hydrogen bonds in the quadruplex were broken, while hydrogen exchange for a specific imino proton should not be dependent on exchange of other protons. The detailed study of the conformational exchange will be reported elsewhere.

4. Conclusion

We have studied the hydrogen exchange rates of imino protons of the thrombin-binding DNA aptamer in the presence of Sr^{2+}. The eight iminos in the quadruplex showed different exchange rates, although the difference was small. The iminos in the TT loops were most difficult to exchange. The iminos outside any loops were easiest to exchange. The imino inside the TGT loop exchanged at a medium rate. The folding and unfolding of the quadruplex mechanism is thus proposed. When folding, the DNA at first folded two TT loops, then the TGT loop, and at last the three loops folded into a compact quadruplex. The unfolding process was just backward. Firstly, the quadruplex broke all hydrogen bonds outside loops, then broke the hydrogen bonds inside the TGT loop and finally broke the hydrogen bonds inside the TT loops. Our study demonstrated that the TGT loop was less stable than the TT loops in the quadruplex.

References

[1] M. Erard, E. Burggraf, J. Pouyet, Folding and unfolding of the core particle DNA are processes faster than millisecond, FEBS Lett. 149 (1982) 55–58.
[2] J. Jeener, B.H. Meier, P. Bachman, R.R. Ernst, Investigation of exchange processes by two-dimensional NMR spectroscopy, J. Chem. Phys. 71 (1979) 4546–4553.
[3] I.M. Russu, Probing site-specific energetics in proteins and nucleic acids by hydrogen exchange and nuclear magnetic resonance spectroscopy, Methods Enzymol. 379 (2004) 152–175.
[4] L. Zhou, M. Rajabzadeh, D.D. Traficante, B.S.P. Cho, Conformational heterogeneity of arylamine-modified DNA: F-19 NMR evidence, J. Am. Chem. Soc. 119 (1997) 5384–5389.
[5] F.J.J. Overmars, C. Altona, NMR study of the exchange rate between two stacked conformers of a model holliday junction, J. Mol. Biol. 272 (1997) 519–524.
[6] A.T. Phan, D.J. Patel, Two-repeat human telomeric d(TAGGGTTAGGGT) sequence forms interconverting parallel and antiparallel G-quadruplexes in solution: distinct topologies, thermodynamic properties, and folding/unfolding kinetics, J. Am. Chem. Soc. 125 (2003) 15021–15027.
[7] L.C. Bock, L.C. Griffin, J.A. Latham, E.H. Vermaas, J.J. Toole, Selection of single-stranded DNA molecules that bind and inhibit human thrombin, Nature 355 (1992) 564–566.
[8] K. Padmanabhan, K.P. Padmanabhan, J.D. Ferrara, J.E. Sadler, A. Tulinsky, The structure of alpha-thrombin inhibited by a 15-mer single stranded DNA aptamer, J. Biol. Chem. 268 (1993) 17651–17654.
[9] J.Y. Wang, S.H. Krawczyk, N. Bischofberger, S. Swaminathan, P.H. Bolton, The tertiary structure of a DNA aptamer which binds to and inhibits thrombin determines activity, Biochemistry 31 (1993) 11285–11292.
[10] J.Y. Wang, S. McCurdy, R.G. Shea, S. Swaminathan, P.H. Bolton, A DNA aptamer which binds to and inhibits thrombin exhibits a new structural motif for DNA, Biochemistry 32 (1993) 1899–1904.
[11] R.F. Macaya, P. Schultze, F.W. Smith, J.A. Roe, J. Feigon, Thrombin-binding DNA aptamer forms a unimoleculr quadruplex structure in solution, Proc. Natl. Acad. Sci. U. S. A. 90 (1993) 3745–3749.
[12] P. Schultze, R.F. Macaya, J. Feigon, Three-dimensional solution structure of the thrombin-binding DNA aptamer d(GGTTGGTGTGGTTGG), J. Mol. Biol. 235 (1994) 1532–1547.
[13] K. Padmanabhan, A. Tulinsky, An ambiguous structure of a DNA 15-mer thrombin complex, Acta Crystallogr., D Biol. Crystallogr. 52 (1996) 272–282.
[14] J.A. Kelly, J. Feigon, T.O. Yeates, Reconciliation of the X-ray and NMR structures of the thrombin-binding aptamer, J. Mol. Biol. 256 (1996) 417–422.
[15] V.M. Marathias, K.Y. Wang, S. Kumar, T.Q. Pham, S. Swaminathan, P.H. Bolton, Determination of the number and location of the manganese binding sites of DNA quadruplexes in solution by EPR and NMR in the presence and absence of thrombin, J. Mol. Biol. 260 (1996) 378–394.
[16] V.M. Marathias, P.H. Bolton, Structure of potassium-saturated, 2:1, and intermediate, 1:1, forms of quadruplex DNA, Nucleic Acids Res. 28 (2000) 1969–1977.
[17] I. Smirnov, R.H. Shafer, Lead is unusually effective in sequence-specific folding of DNA, J. Mol. Biol. 296 (2000) 1–5.
[18] B.I. Kankia, L.A. Marky, Folding of the thrombin aptamer into a G-quadruplex with Sr^{2+}: stability, heat and hydration, J. Am. Chem. Soc. 31 (2001) 10799–10804.
[19] I.V. Smirnov, F.W. KOtch, I.J. Pickering, J.T. Davis, R.H. Shafer, Pb EXAFS studies on DNA quadruplexes: identification of metal ion binding site, Biochemistry 41 (2002) 12133–12139.
[20] M. Vairamani, M.L. Gross, G-quadruplex formation of thrombin-binding aptamer detected by electrospray ionization mass spectrometry, J. Am. Chem. Soc. 125 (2003) 42–43.
[21] N. Kumar, S. Maiti, Quadruplex to Watson–Crick duplex transition of the thrombin binding aptamer: a fluorescence resonance energy transfer study, Biochem. Biophys. Res. Commun. 319 (2004) 759–767.
[22] X.A. Mao, L.A. Marky, W.H. Gmeiner, NMR structure of the thrombin-binding DNA aptamer stabilized by Sr^{2+}, J. Biomol. Struct. Dyn. 22 (2004) 25–33.
[23] S. Neidle, M.A. Read, G-quadruplexes as therapeutic targets, Biopolymers 56 (2000) 195–208.
[24] S. Macura, R.R. Ernst, Elucidation of cross relaxation in liquids by two dimensional NMR spectroscopy, Mol. Phys. 41 (1980) 95–117.
[25] M. Piotto, V. Saudek, V. Sklenar, Gradient-tailored water suppression for single quantum NMR spectroscopy of aqueous solutions, J. Biomol. NMR 2 (1992) 661–665.
[26] A. Bax, D.G. Davis, Practical aspects of two-dimensional transverse NOE spectroscopy, J. Magn. Reson. 63 (1985) 207–213.
[27] S.W. Englander, J.J. Englander, Structure and energy change in hemoglobin by hydrogen exchange labeling, Methods Enzymol. 232 (1994) 26–42.